Pergamon

PII: S0191–8141(98)00022–4

Journal of Structural Geology, Vol. 20, No. 7, pp. 937 to 944, 1998

0191-8141/98 $19.00 + 0.00

Magnetite grain shape fabric and distribution anisotropy vs rock magnetic fabric: a three-dimensional case study

V. GRÉGOIRE, J. DARROZES, P. GAILLOT and A. NÉDÉLEC*

Pétrophysique et Tectonique, UMR 5563 CNRS, Université Paul-Sabatier, 38 rue des 36-Ponts, 31400 Toulouse, France

and

P. LAUNEAU

Pétrologie structurale, UPRES-EA 2156, Université de Nantes, 2 rue de la Houssinière, 44072 Nantes, France

(*Received* 24 *April* 1997; *accepted in revised form* 18 *February* 1998)

Abstract—Shape fabric and distribution anisotropy of magnetite grains in a highly ferromagnetic (*s.l.*) syenite are determined for three mutually perpendicular planes on about 600 magnetite grains. The grains are lenticular with an average aspect ratio of about 2.0. Their preferred orientation, determined by the inertia tensor method, is consistent with the principal directions of the magnetic susceptibility ellipsoid and the axial ratios of the magnetic fabric ellipses are very close to those of the shape fabric ellipses (e.g. 1.41 and 1.39 in the section plane perpendicular to the magnetic foliation and parallel to the magnetic lineation). The anisotropic wavelet transform can detect and quantify the anisotropic distribution of the magnetite grains which are located interstitially along the feldspar grain boundaries. This anisotropic distribution has no noticeable effect on the rock's anisotropy of magnetic susceptibility (AMS), since only a few percent of grains are close enough to interact magnetically. Therefore, it is realistic to consider that the AMS of ferromagnetic granitic rocks originates mainly from the shape fabric of anisotropic magnetite grains and a close correlation between the magnetic fabric and the magnetite grain shape fabric is expected.

INTRODUCTION

Low-field anisotropy of magnetic susceptibility (AMS), or magnetic fabric, is an excellent tool for unravelling the petrofabrics of igneous rocks (e.g. Ellwood and Whitney, 1980; Hrouda, 1982; Borradaile, 1988; Borradaile and Henry, 1997; Bouchez, 1997). In magnetite-bearing rocks, both shape fabric and the distribution anisotropy of magnetite grains have been advocated to play a major role in the resulting rock AMS (Hargraves *et al.*, 1991; Stephenson, 1994; Archanjo *et al.*, 1995; Cañón-Tapia, 1996). Grégoire *et al.* (1995) experimentally verified that magnetic interaction between two magnetite grains occurs when the centre-to-centre distance between the grains is less than the mean grain size. They suggested that the magnetic interaction may either reduce or enhance the magnitude of the whole-rock anisotropy depending on the distribution anisotropy of the magnetite grains. However, the importance of this contribution is still a matter of speculation owing to the lack of detailed textural investigations. In the only case study to date, Archanjo *et al.* (1995) concluded that the magnetic fabric of a magnetite-bearing granite is controlled mainly by the preferred shape orientation of magnetite grains, although magnetic interactions between cluster grains cannot be excluded. To get a more definitive appreciation, we selected a syenite with a high magnetite content of ~3% and carried out the three-dimensional characterisation of shape, shape fabric and distribution of its magnetite grains. The origin and significance of the whole-rock AMS are then considered using this data set.

MATERIALS AND METHODS

The selected rock is a quartz syenite from a several hundred metre-thick moderately dipping sheet-like intrusion in Madagascar. Detailed mineralogy and geochemistry can be found in Nédélec *et al.* (1995) for sample number MG 93. The studied rock displays a conspicuous foliation, acquired under near-solidus conditions during syntectonic emplacement under a high geothermal gradient. The foliation arises from a crude preferred shape orientation of the perthitic alkali feldspars and from some compositional layering. A well-defined magnetic lineation is determined also by the AMS measurements. The iron-rich minerals are clinopyroxene, hornblende and oxides. The oxide minerals represent about 3% of the volume of the rock. They are magnetite and ilmenite in textural equilibrium so that the crystals are generally devoid of exsolutions. Magnetite is much more abundant, amounting to nearly 90% of the oxide minerals. This is a very high

*Author to whom correspondence should be addressed.

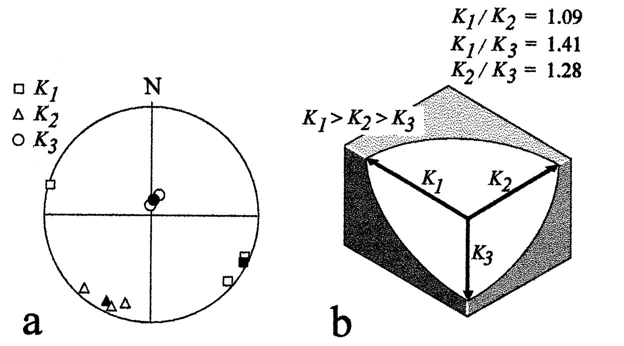

Fig. 1. (a) Stereographic plot (lower hemisphere) with projections of the AMS principal axes ($K_1 \geq K_2 \geq K_3$); open symbols: specimens, filled symbols: averages. (b) Three-dimensional representation of the AMS ellipsoid principal axes for the studied rock.

magnetite content for a granitic rock where distribution anisotropy (if any) could produce the highest magnetic interactions. AMS measurements were made with a Kappabridge KLY-2 (AGICO Brno) susceptibility meter working at 4×10^{-4} T and 920 Hz with a detection limit of about 4×10^{-8} SI. Three oriented cylindrical specimens, each with a volume of ~10.8 cm^3, were used. Their mean susceptibility is 5.77×10^{-2} SI. This rather high value (for a granitic rock) is related to the high magnetite content of the syenite (Nagata, 1953). The directions of the principal axes ($K_1 \geq K_2 \geq K_3$) of the magnetic susceptibility ellipsoid are fairly constant in the three specimens (Fig. 1a) and the average ellipsoid is oblate (Fig. 1b).

Oriented thin sections were cut from the same sample, parallel to the three reference planes (K_1K_2, K_1K_3, K_2K_3) of the magnetic susceptibility ellipsoid (Fig. 2). The total number of sections amounts to 18 (6×3). Three-dimensional textural information was interpolated from these orthogonal two-dimensional sections. Oxide minerals were identified visually as opaques using a Petroscope (Minox GmbH Giessen) and outlined manually prior to digitising. Thus, around 600 oxide grains were studied. As this was done in transmitted light, magnetite and ilmenite could not be distinguished so the oxide phase was considered mixed in the study. Given that magnetite is by far the most abundant oxide, the results yielded by the oxide phase constitute a good approximation for the magnetite phase and, hence, may be compared with the AMS properties of the rock. Magnetite is essentially an interstitial phase in the studied syenite. Most of the magnetite grains are xenomorphic, even if one or two crystalline faces are well developed in some cases.

The grain size and shape fabric data were extracted out of the digitised images by the OPF ('Orientation Préférentielle de Forme', i.e. Preferred Shape Orientation) program of Launeau (1997) using the inertia tensor method (Jähne, 1995) for determination of the size, shape and fabric of the grains, and the wavelet program of Darrozes *et al.* (1997) for determination of their spatial distribution. The wavelets, allowing for both local and multi-scale analysis, are used to dissociate and quantify different levels of organisation of complex systems (Meyer and Roques, 1993). Applied to rock fabric analysis, the two-dimensional anisotropic wavelet transform detects organised patterns due to a non-uniform spatial distribution of minerals. It discriminates objects and clusters depending of their area, shape, orientation and position (Gaillot *et al.*, 1997). The analysing wavelet is an anisotropic filter called 'Mexican Hat', constructed to unravel the expected entities. As shown in Fig. 3, the geometry of the filter is determined by four parameters: the wavelet's short axis a (also called the wavelet resolution), the wavelet shape ratio σ, the azimuth θ of the long axis of the wavelet, and the location vector x. At each point in the binary image (256×256 pixels), the wavelet transform coefficient C is calculated using the software developed by Darrozes *et al.* (1997). This coefficient is a local indicator of the presence of organised structures of a given scale. Thus, weak coefficients are associated with areas of constant gradient or of other levels of organisation, and strong coefficients point out the structures of interest.

GRAIN SHAPE

The length l and aspect ratio r of each grain were calculated using the inertia tensor method. The results for the three orthogonal sections (K_1K_3, K_2K_3 and K_1K_2) are given in Fig. 4. The 0.0–0.2 mm class is empty because these grains are too small to be properly analysed. The frequency histograms of length measurements are unimodal and present a main class size ranging from 0.4 to 0.6 mm in all three sections. The average lengths are 0.75 mm $\pm$ 0.32 mm (σ), 0.73 mm $\pm$ 0.29 mm (σ) and 0.70 mm $\pm$ 0.29 mm (σ) in sections K_1K_3, K_2K_3 and K_1K_2, respectively. These values are slightly higher than the peak values due to a large number of very long grains or grain clusters. The frequency histograms of the aspect ratios display a main class (18–25% of the grains) for shape ratios r ranging between 1.75 and 2.00 in K_1K_3 section and between 1.50 and 1.75 in K_2K_3 and K_1K_2 sections. Classes with higher shape ratios are also well represented; hence, the average aspect ratios are about 1.90. The highest values for l and r do not necessarily correspond to individual grains, but rather represent aggregates of grains that could not be analysed separately.

In the K_1K_3 and K_2K_3 sections, the average length and aspect ratios are nearly equal, characterising lenticular grains. In this case, the mean aspect ratio in the K_1K_2 sections would be about 1.00, whereas the measured ratios are noticeably higher. The higher ratios result from the grains being co-zonally oriented around the K_1 direction. This interpretation is strengthened by the fact that the K_1 direction is well defined by AMS measurements.

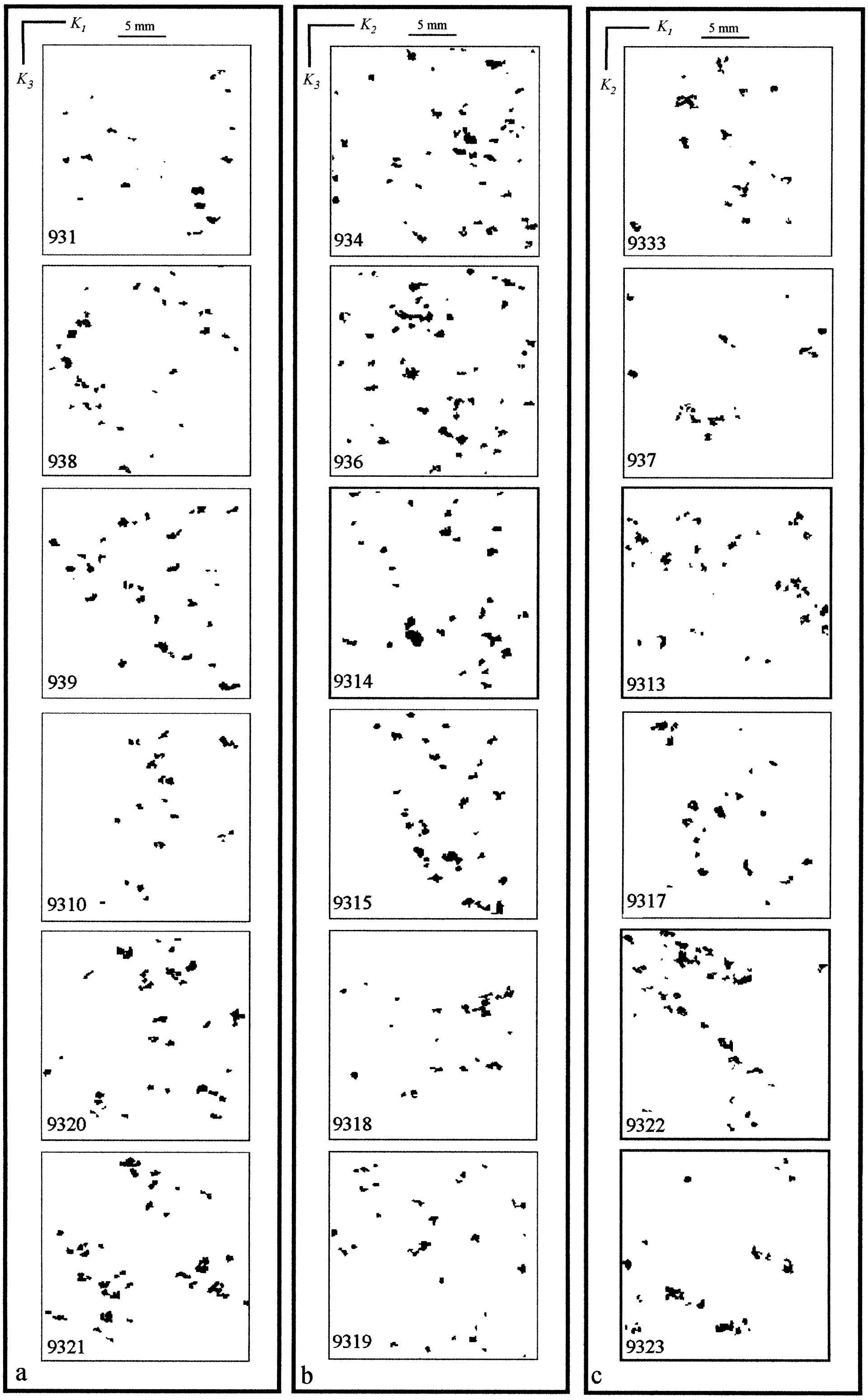

Fig. 2. Digitised oriented thin sections in: (a) K_1K_3; (b) K_2K_3; and (c) K_1K_2 planes, respectively.

GRAIN PREFERRED ORIENTATION

The preferred orientation of grain populations, or shape fabric, was also studied in the three orthogonal planes K_1K_3, K_2K_3 and K_1K_2. The orientation of the long axis and mean axial ratio R of the ellipses representing the population fabrics were calculated by the SPO program from the average inertia tensor of the grain shapes. The shape fabric ellipses are presented in Fig. 5 together with the magnetic fabric ellipses for each reference plane. The axes of the fabric ellipses fit closely with the corresponding axes of the AMS

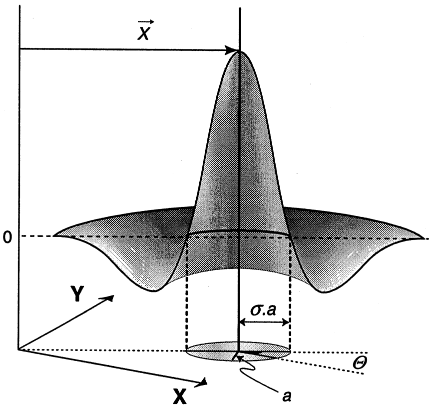

Fig. 3. Anisotropic 'Mexican Hat', $\psi_r(x, a, a\ \sigma, \theta)$, in which the resolution is a, the shape ratio is σ, the orientation is θ, and the location is $\vec{x}$.

ellipses, as the average angle departures from K_1, K_2 and K_3 do not exceed 3°. These results fit better than those of Archanjo *et al.* (1995) because about 200 grains were measured in each reference plane, whereas individual thin sections may yield higher discrepancies with maximum angle departures of 10, 14 and 28° in the K_1K_3, K_2K_3 and K_1K_2 planes, respectively. AMS measurements always involve rock volumes where hundreds or thousands of grains are measured, so that AMS is obviously a powerful structural tool for determining lineations (K_1) and foliation poles (K_3) of mineral fabrics in ferromagnetic rocks.

The average axial ratios R of the shape fabric ellipses are 1.39 ± 0.13 (σ), 1.28 ± 0.08 (σ) and 1.08 ± 0.07 (σ) in the sections K_1K_3, K_2K_3 and K_1K_2, respectively. Not surprisingly, these ratios are in agreement with the oblate shape of the grains.

Comparison of these axial ratios with those of the AMS ellipses shows that the degree of anisotropy in the shape fabric of the magnetite grains is very close to the degree of anisotropy of the magnetic fabric in the three mutually-perpendicular sections. A linear correlation between the intensities of both fabrics is also suggested by these results. Hence, magnetite grain populations appear to be characterized by a property similar to the one of individual magnetite grains that display a linear correlation between their aspect ratio and their anisotropy of magnetic susceptibility (Uyeda *et al.*, 1963; Grégoire *et al.*, 1995).

To be sure that there is a good correlation between the AMS ellipsoid and the shape fabric ellipsoid, we need to know how the grains are distributed, i.e. to explore the spatial configurations where magnetic interactions may occur, even if they partially compensate themselves.

GRAIN DISTRIBUTION

One aim of the present study is to try to recognise particular configurations of fabric caused by larger features such as grain aggregates or grain alignments.

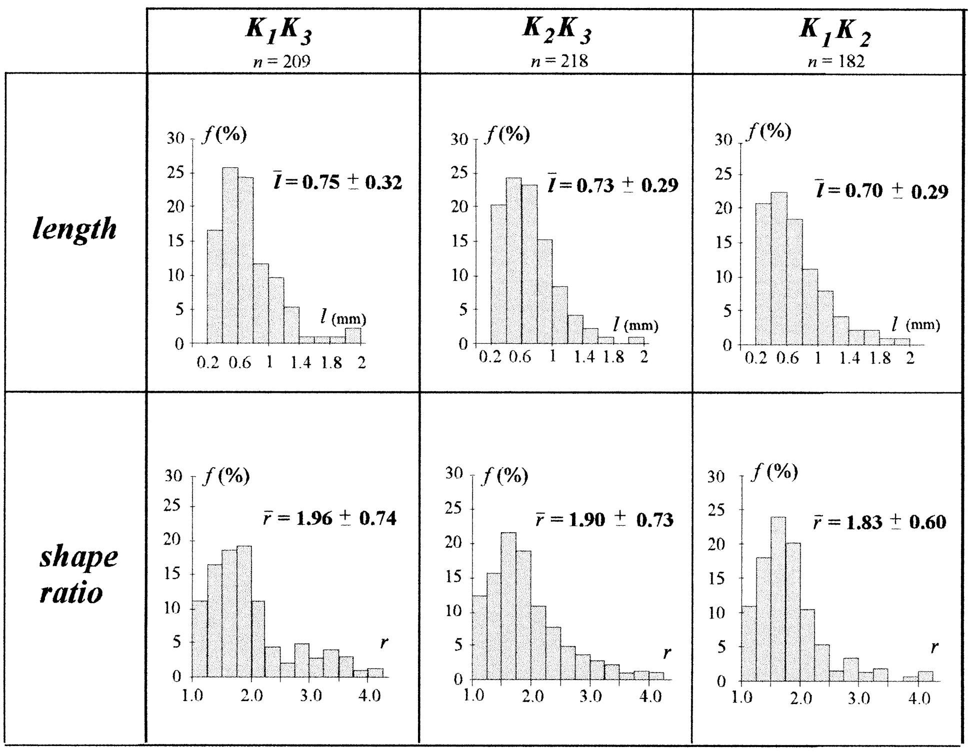

Fig. 4. Frequency histograms of the length l (averages and mean standard deviations) and shape ratio r (averages and standard deviations) of the magnetite grains in the K_1K_3, K_2K_3 and K_1K_2 section planes.

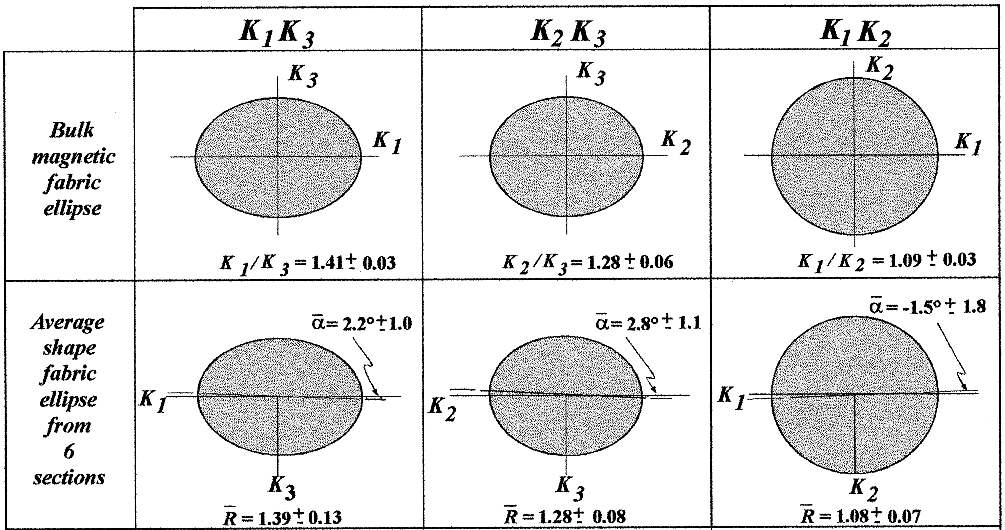

Detailed results of each section	Sections	α°	R	Sections	α°	R	Sections	α°	R
	931	-3	1.54	934	14	1.39	933	25	1.24
	938	1	1.31	936	3	1.33	937	22	1.11
	939	-10	1.62	9314	7	1.27	9313	-6	1.04
	9310	4	1.29	9315	-9	1.37	9317	-28	1.20
	9320	-8	1.33	9318	-5	1.17	9322	-23	1.18
	9321	1	1.35	9319	6	1.23	9323	13	1.10

Fig. 5. Magnetic fabric and shape fabric ellipses for the three section planes (K_1K_3, K_2K_3 and K_1K_2); averages, standard deviations and detailed results are obtained by the OPF program using the inertia tensor method.

Magnetic interactions between neighbouring grains is supported by testing the alignments between grains whose centre-to-centre distance is less than a critical value (Grégoire *et al.*, 1995; Cañón-Tapia, 1996). Grégoire *et al.* (1995) studied experimentally the magnetic interactions between adjacent magnetite grains. The results of their two-grain experiments strongly depend on the spatial configurations of the nearby interacting grains, namely 'side-by-side' and 'aligned' configurations (Fig. 6). In the first case, the direction of the easiest magnetization is rotated by 90°, when the grain interspace is less than one grain size. In the second case, the anisotropy degree becomes higher, but there is no change of the orientation of the magnetic axes. Cañón-Tapia (1996) calculated the magnetic interactions occurring in model one-, two- and three-dimensional arrays of anisotropic magnetic particles. He demonstrated that the resulting magnetic fabric may be modified in orientation and intensity when the intergrain distance is generally less than one grain size. More precisely, he pointed out that the effect of magnetic interactions becomes significant only if the intergrain distance is less than 0.25 grain size. Otherwise, magnetic interactions are negligible if the intergrain distance is more than 1.5 grain size.

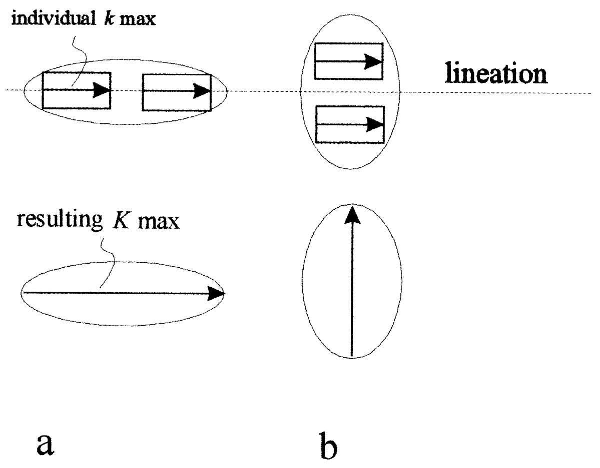

Fig. 6. Typical configurations of interacting magnetite grains showing the: (a) 'aligned'; and (b) 'side-by-side' configurations of Grégoire *et al.* (1995). k_{max} is the maximum magnetic susceptibility of the grain and K_{max} represents the maximum magnetic susceptibility of interacting grains (not to scale).

The wavelet method can recognise configurations where the magnetite grains are closer together than a critical distance. The wavelet parameters are selected in order to detect spatial configurations of paired interacting grains as shown in Fig. 7. Assuming a mean grain size l of 0.73 mm, the chosen wavelet is characterised by its resolution $a = 0.22$ mm and its shape ratio $\sigma = 4$. Wavelet coefficients were thresholded in order to determine paired grains separated by ≤1 average grain size (for $C \geq 0.22$) and separated by ≤0.25 grain size (for $C \geq 0.42$). Because the wavelet resolution, the wavelet shape ratio and the coefficient threshold are the same for all analysed images, the results can be accumulated for each section plane.

The results are presented as rose diagrams for each section plane in Fig. 8. Interacting paired grains (clusters or alignments) were recognised in both cases, pointing to the existence of an anisotropic distribution of the magnetite grains. In some cases, their preferred

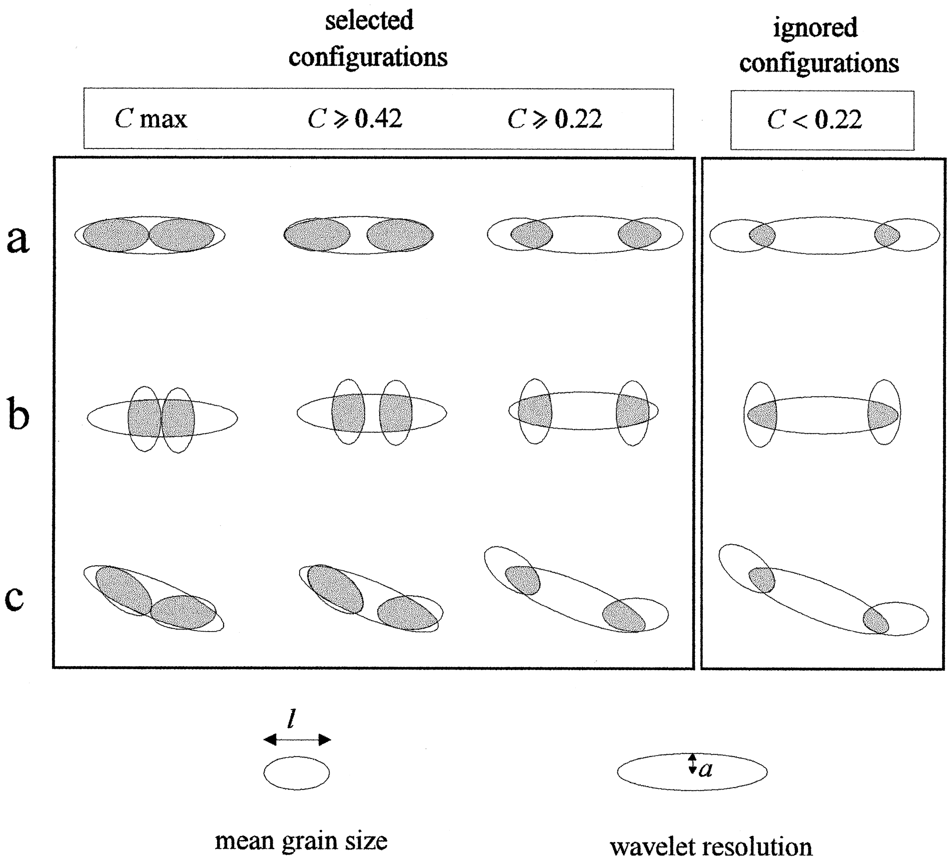

Fig. 7. Selected wavelet with coefficient thresholds enabling detection of: 'aligned', 'side-by-side' and intermediate configurations corresponding to intergrain distances of interest.

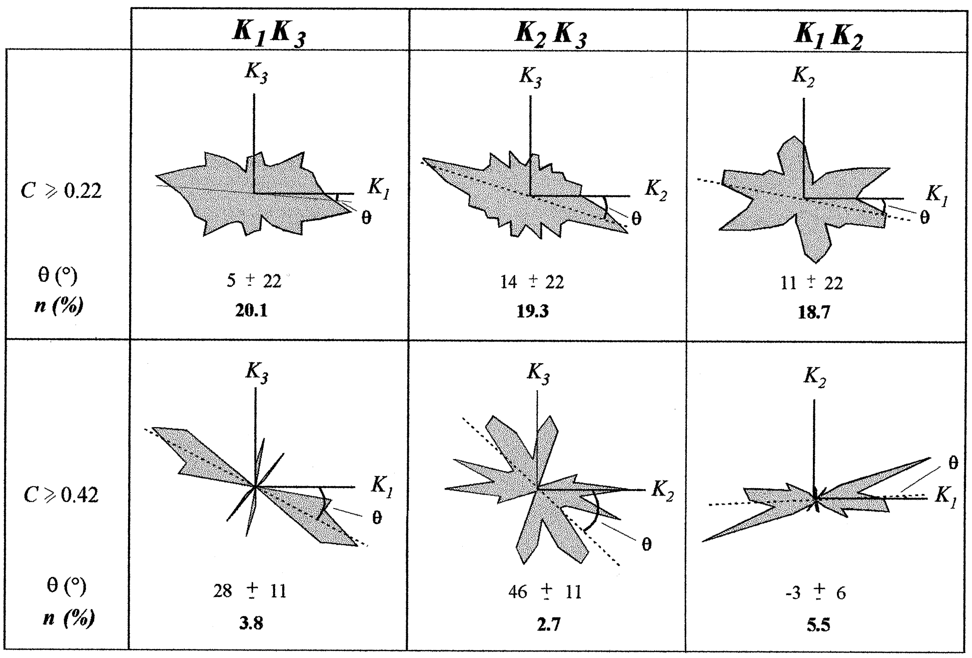

Fig. 8. Rose diagrams for the interacting paired grains (aggregates) in the K_1K_3, K_2K_3 and K_1K_2 section planes; θ is the mean orientation of the aggregates and n is the percentage of grains involved in the pairs or aggregates. Results for the two different coefficient thresholds are not to the same scale.

orientations differ from the orientation of the magnetic axes and, hence, from the preferred orientations of individual grains that are nearly coaxial with the magnetic axes (Fig. 5). For instance, three different orientations are recognised in the K_1K_2 section for $C \geq 0.22$ and in the K_2K_3 section for $C \geq 0.42$. The resulting mean angle θ is less than 15° in the three section planes for $C \geq 0.22$, but it amounts to 46.3° in the K_2K_3 section for $C \geq 0.42$. In this last case, the orientation of the local magnetic ellipsoids may be different from the bulk magnetic fabric, as a result of magnetic interactions. Nevertheless, the percentage n of grains close enough to interact magnetically in a significant way is quite small. This percentage is less than 6% for $C \geq 0.42$ (i.e. intergrain distance $\leq$0.25 grain size).

DISCUSSION AND CONCLUSIONS

The present study provides a thorough investigation of the size, shape and spatial distribution of the magnetite grains in the selected syenite. Magnetite grains are dominantly oblate, with an average length of 0.76 mm and a shape ratio around 1.9. This pronounced shape anisotropy of the grains results from their crystallisation in interstices and also possibly from some plastic behaviour at near solidus temperatures (Housen *et al*., 1995), given that the studied rock is syntectonic.

Shape fabric data in three orthogonal planes show that the AMS ellipsoid and the magnetite shape fabric ellipsoid are coaxial and that the ratios of their principal axes are nearly equal in the selected syenite. This very good correlation is established by considering a large number of grains (around 200 in each section plane). Archanjo *et al*. (1995) did not establish such a close correlation for the anisotropy magnitudes (despite a good agreement between their directions) and suggested that this could result from magnetic interaction between magnetite grains forming clusters. We think that another explanation of their results may be the low number of grains studied (less than 100 in each section plane).

The wavelet method has unravelled the anisotropic distribution of the magnetite grains. This new approach allows us to determine the preferred orientations of grain aggregates and to estimate that around 20% of the grains are distant by $\leq$1 mean grain size and less than 6% of the grains are distant by $\leq$0.25 mean grain size. It must be noted that these results were derived from orthogonal two-dimensional sections and not from an actual three-dimensional investigation, as could be obtained by high-resolution X-ray tomography (Denison *et al*., 1997). Therefore, our results are only estimates of the actual spatial distribution. Nevertheless, the existence of a distribution anisotropy of the magnetite grains appears well established and probably arises from the interstitial location of the magnetite grains that crystallised after akali feldspar, the main mineral phase in the syenite. Consequently, magnetic interactions occur locally, at least for a few percent of the grains. However, their contribution is too weak to have a recognisable effect on the AMS and the shape fabric of anisotropic magnetite grains remains the major contribution to the magnetic fabric, since both fabrics are closely related in orientations and intensities. This is at variance with the conclusion of Cañón-Tapia (1996) that emphasised the effect of magnetic interaction, i.e. the effect of grain distribution with respect to grain orientation in igneous rocks containing more than 1 vol.% of magnetite. Thus, we maintain that AMS measurements can be used with confidence to infer the mineral fabric in ferromagnetic granitic rocks.

Acknowledgements—The authors are indebted to C. Cavaré-Hester and A. M. Roquet for technical assistance. Discussions with J. L. Bouchez and M. de Saint Blanquat are gratefully acknowledged. Critical comments by R. Panozzo-Heilbronner and P. Rochette on an earlier draft contributed significantly to the improvement of the present paper. B. Housen and D. T. A. Symons are warmly thanked for their detailed reviews.

REFERENCES

Archanjo, C. J., Launeau, P. and Bouchez, J. L. (1995) Magnetic fabrics vs magnetite and biotite shape fabrics of the magnetite-bearing granite pluton of Gameleiras (Northeast Brazil). *Physics of the Earth and Planetary Interiors* **89,** 63–75.

Borradaile, G. J. (1988) Magnetic susceptibility, petrofabrics and strain. *Tectonophysics* **156,** 1–20.

Borradaile, G. J. and Henry, B. (1997) Tectonic applications of magnetic susceptibility and its anisotropy. *Earth Sciences Review* **42,** 49–93.

Bouchez, J. L. (1997) Granite is never isotropic: an introduction to AMS studies of granitic rocks. In *Granite: From Segregation of Melt to Emplacement Fabrics*, eds J. L. Bouchez, D. Hutton and W. E. Stephens, pp. 95–112. Kluwer Academic Publishers, Dordrecht.

Cañón-Tapia, E. (1996) Single-grain versus distribution anisotropy: a simple three-dimensional model. *Physics of the Earth and Planetary Interiors* **94,** 149–158.

Darrozes, J., Gaillot, P., Saint Blanquat (de), M. and Bouchez, J. L. (1997) Software for multi-scale image analysis: the normalised optimised anisotropic wavelet coefficient method. *Computers and Geosciences* **23,** 889–895.

Denison, C., Carlson, W. D. and Ketcham, R. A. (1997) Three-dimensional quantitative textural analysis of metamorphic rocks using high-resolution computed X-ray tomography: Part I. Methods and techniques. *Journal of Metamorphic Geology* **15,** 29–44.

Ellwood, B. B. and Whitney, J. A. (1980) Magnetic fabric of the Elberton granite, Northeast Georgia. *Journal of Geophysical Research* **85,** 1481–1486.

Gaillot, P., Darrozes, J., Saint Blanquat (de), M. and Ouillon, G. (1997) The normalised optimised anisotropic wavelet coefficient (NOAWC) method: an image processing tool for multi-scale analysis of rock fabric. *Geophysical Research Letters* **24,** 1819–1822.

Grégoire, V., Saint Blanquat (de), M., Nédélec, A. and Bouchez, J. L. (1995) Shape anisotropy versus magnetic interactions of magnetite grains: experiments and application to AMS in granitic rocks. *Geophysical Research Letters* **22,** 2765–2768.

Hargraves, R. B., Johnson, D. and Chan, C. Y. (1991) Distribution anisotropy: the cause of AMS in igneous rocks? *Geophysical Research Letters* **18,** 2193–2196.

Housen, B., van der Pluijm, B. A. and Essene, E. J. (1995) Plastic behaviour of magnetite and high strains obtained from magnetic fabrics in the Parry Sound shear zone, Ontario Grenville Province. *Journal of Structural Geology* **17,** 265–278.

Hrouda, F. (1982) Magnetic anisotropy of rocks and its application in geology and geophysics. *Geophysical Survey* **5,** 37–82.

Jähne, B. (1995) *Digital Image Processing, Concepts, Algorithms and Scientific Applications*. Springer-Verlag, Berlin.

Launeau, P. (1997) Measurement of 3D anisotropy by analysis of three orthogonal images using quadratic shape tensors. In *European Union of Geosciences*. 376. Strasbourg, **9**.

Meyer, Y. and Roques, S. (1993) *Progress in Wavelet Analysis and Applications*. Frontières, Paris.

Nagata, T. (1953) *Rock-Magnetism*. Maruzen Company, Tokyo.

Nédélec, A., Stephens, W. E. and Fallick, A. E. (1995) The Panafrican stratoid granites of Madagascar: alkaline magmatism in a post-collisional extensional setting. *Journal of Petrology* **36,** 1367–1391.

Stephenson, A. (1994) Distribution anisotropy: two simple models for magnetic lineation and foliation. *Physics of the Earth and Planetary Interiors* **82,** 49–53.

Uyeda, S., Fuller, M. D., Belshe, J. C. and Girdler, R. W. (1963) Anisotropy of magnetic susceptibility of rocks and minerals. *Journal of Geophysical Research* **68,** 279–291.